Fermilab Library
0 1160 0006175 8

DOE-40427-37-N91

FERMILAB
FEB 14 1992
LIBRARY

Solar Neutrinos: Theoretical Status

W.C. Haxton

National Institute for Nuclear Theory, HN-12 and Department of Physics, FM-15

University of Washington, Seattle, Washington 98195

Invited talk at Current Topics in Astrofundamental Physics

Ettore Majorana Centre, Erice, Italy

September 1-8, 1991

and

Second International Workshop on Theoretical and Phenomenological

Aspects of Underground Physics

Toledo, Spain, September 9-13, 1991

PREPARED FOR THE U.S. DEPARTMENT OF ENERGY

This report was prepared as an account of work sponsored by the United States Government. Neither the United States nor the United States Department of Energy, nor any of their employees, nor any of their contractors, subcontractors, or their employees, makes any warranty, express or implied, or assumes any legal liability or responsibility for the product or process disclosed, or represents that its use would not infringe privately-owned rights.

By acceptance of this article, the publisher and/or recipient acknowledges the U.S. Government's right to retain a nonexclusive, royalty-free license in and to any copyright covering this paper.

ROUTE TO
NAME
LOCATION

DOE-ER-40427-37-N91

SOLAR NEUTRINOS: THEORETICAL STATUS

W. C. HAXTON
National Institute for Nuclear Theory, HN-12 and Department of Physics, FM-15
University of Washington, Seattle, Washington 98195

ABSTRACT

I review the standard solar model, the disparities between its predictions and the solar neutrino flux measurements of the Homestake and Kamioka II collaborations, and possible particle physics resolutions of this puzzle. The effects of matter, including density fluctuations and turbulence, on solar neutrino oscillations are explained by building analogies with more familiar atomic physics phenomena. These and other mechanisms are considered as possible explanations for time variations in the solar neutrino flux. Finally, I consider possible outcomes and implications of the SAGE/GALLEX gallium experiments.

The solar neutrino flux presents us with unique opportunities to search for new phenomena in weak interactions. If flavor mixing exists, the sun can serve as a marvelous regenerator, greatly enhancing the effects of neutrino oscillations.[1,2,3] If the neutrino has a magnetic moment, passage through the intense fields in the sun's convective envelope can reverse the neutrino's helicity.[4,5,6,7]

Solar neutrinos also serve as an important test of our understanding of main-sequence stellar evolution: can the standard solar model[8] account for observed properties of the sun? In detail the answer to this question must be no: for instance, we do not understand the complicated surface activity that governs the 11-year solar cycle. Yet the standard solar model does make definite predictions about the temperature and composition of the solar core, where the neutrinos are produced. If we can measure the flux and spectra of the various neutrino sources, these predictions can be put to a rigorous test.

There are four basic assumptions[8] in the standard solar model:

- The sun evolves in hydrostatic equilibrium: there is a local balance between the gravitational force and the pressure gradient. To describe this condition in detail one must specify the equation of state as a function of temperature, density, and composition. It is believed that an ideal gas EOS is a good approximation.

- One must specify the mechanisms for energy transport. While the solar envelope is convective, radiation dominates in the core region where energy and neutrinos

are produced. Thus neutrino flux predictions depend on a correct description of the radiative opacity as a function of the (changing) chemical composition of the core.

• The thermonuclear reaction chains that generate solar energy must be described. The standard model predicts that over 98% of this energy is derived from the conversion four protons into ^{4}He (see Table I)

$$4p \rightarrow {}^4\mathrm{He} + 2e^+ + 2\nu_e + \mathrm{energy},$$

with the CNO cycle contributing the remaining 2%. The sun is a very large but very slow reactor: the core temperature, $T_c \sim 1.5 \cdot 10^7$ K, results in typical center-of-mass reaction energies of 10-20 keV, far smaller than the Coulomb barriers inhibiting charged-particle nuclear reactions. Thus reaction rates are small, and one must depend on extrapolations[9] of laboratory data taken at much higher energies ($\gtrsim 50$ keV) to determine the needed cross sections.

Table I. The pp chain. Branching percentages for competing reactions are taken from the standard model calculations of Bahcall and Ulrich.[8]

Reactions	Branching %	E_ν^{max}(MeV)	Comments
I. $p+p \rightarrow {}^2H+e^+ +\nu$	99.75	0.42	
or $p+e^- +p \rightarrow {}^2H+\nu$	0.25	1.44	
II. ${}^2H+p \rightarrow {}^3He+\gamma$	100		
III. ${}^3He+{}^3He \rightarrow {}^4He+2p$	86		ppI Termination
or ${}^3He+{}^4He \rightarrow {}^7Be+\gamma$	14		
IV. ${}^7Be+e^- \rightarrow {}^7Li+\nu$		0.86 (90%) 0.38 (10%)	
${}^7Li+p \rightarrow 2\ {}^4He$	99.89		ppII Termination
or ${}^7Be+p \rightarrow {}^8B+\gamma$			
${}^8B \rightarrow {}^8Be^* +e^+ +\nu$	0.11	14.06	ppIII Termination

• One must satisfy the solar boundary conditions, e.g., produce a model with the correct radius, mass, and present luminosity. An important assumption of the standard solar model is that the sun was highly convective, and therefore uniform in composition, when it first entered the main sequence. It is further assumed that the surface abundances of metals (nuclei with A $\geq$ 5) have been unchanged by subsequent evolution, and thus determine the sun's initial metallicity. The remaining

parameter is the initial ^{4}He/H ratio, which is adjusted to reproduce the present solar luminosity once the solar model is evolved through five billion years of main sequence burning.

The model that emerges describes an evolving sun. As the core's chemical composition changes, the opacity and core temperature rise, producing a 44% luminosity increase over the past five billion years. The ^{8}B solar neutrino flux, the most temperature-dependent component, thus proves to be of relatively recent origin: the predicted flux increases exponentially with time with a doubling period of $\sim$ 0.9 billion years.[10]

The neutrino-producing reactions of the pp chain (and CNO cycle) are summarized in Table II. The first four reactions produce beta decay neutrinos in an allowed Fermi distribution with an endpoint given by E_ν^{max}. (Actually the ^{8}B neutrino flux deviates from an allowed spectrum because the ^{8}B final state populated in this decay is a broad resonance.) The last two reactions produce monoenergetic electron capture neutrinos. The electron capture on ^{7}Be leads to both the ground state (90%) and 478 keV first excited state (10%) of ^{7}Li.

Table II. Summary of the most important neutrino-producing reactions of the pp chain and CNO cycle and their standard model fluxes (from Ref. 8).

Source	Max. neutrino energy (MeV)	Flux (10^{10}/cm^2-8)
$p+p \rightarrow {}^2H+e^+ +\nu$	0.42	6.0
${}^{13}N \rightarrow {}^{13}C+e^+ +\nu$	1.20	$6.1 \cdot 10^{-2}$
${}^{15}O \rightarrow {}^{15}N+e^+ +\nu$	1.73	$5.2 \cdot 10^{-2}$
${}^8B \rightarrow {}^8Be+e^+ +\nu$	$\sim$ 14	$5.8 \cdot 10^{-4}$
${}^7Be+e^- \rightarrow {}^7Li+\nu$	0.86 (90%) 0.38 (10%)	$4.7 \cdot 10^{-1}$
$p+e^- +p \rightarrow {}^2H+\gamma$	1.44	$1.4 \cdot 10^{-2}$

The principal experimental goal in solar neutrino spectroscopy has been to measure the fluxes and spectrum shapes (and perhaps also the flavors) of the pp, ^{7}Be, and ^{8}B neutrinos, as these are the keys to distinguishing the ppI, ppII, and ppIII cycles shown in Table I. The "solar neutrino problem" describes the conflict between the first experimental results in this program, those obtained from the Homestake ^{37}Cl detector, and the predictions of the standard solar model. The theoretical capture rate for ^{37}Cl(ν_e, e)^{37}Ar is 8.1 $\pm$ 2.7 SNU (3σ), according to the calculations of Bahcall-Ulrich[8] and 5.8 $\pm$ 1.3 SNU (1σ), according to Turck-Chiéze *et al.*[11]. [SNU = 10^{-36} captures/^{37}Cl atom/second.] I have adjusted the published

values for Refs. 8 and 11 to take into account the recent, improved ^{37}Cl cross section calibration experiment of Garcia *et al.*[12] The difference between the estimates of Ref. 8 and 11 appear to be understood and are primarily due to variations in input parameters, rather than physics differences in the solar models.[10] In particular, the zero-energy S-factor adopted for ^{7}Be (p, γ) is $S_{17}(0) = 0.0243$ keV-b in Ref. 8 and 0.021 keV-b in Ref. 11. A very recent reanalysis[13] of $S_{17}(0)$ has yielded 0.0224 keV-b, a value between those of Refs. 8 and 11. The experimental capture rate for ^{37}Cl, after two decades of measurements, is about 1/3 of theory, 2.1 ± 0.3 (1σ) SNU. As almost 80% of the rate is due to ^{8}B neutrino capture, one interpretation of this result had been that it is compatible with an absence of high energy neutrinos. However the counting rate for the Kamioka II water Cerenkov detector[14], in which ν - e elastic scattering is employed as a real-time (and direction-sensitive) signal for the interaction of high energy ($\gtrsim 7.5$ MeV or $\gtrsim 9.3$ MeV) neutrinos, is 0.46 ± 0.05 (stat) $\pm$ 0.06 (sys) of the standard solar model, a somewhat less severe deficiency. The Kamioka II detector is sensitive to ν_es and heavy flavor neutrinos, though the cross section for the latter is about 1/6 of the former.

There have been searches for "trivial" solutions of the solar neutrino puzzle: solutions where the essential physics of neutrinos and of the standard solar model is unchanged, but where the input parameters are adjusted. For instance, if, in either the third or fourth steps of the pp chain

$$III\begin{cases} {}^3\mathrm{He} + {}^3\mathrm{He} \rightarrow {}^4\mathrm{He} + p \\ {}^3\mathrm{He} + {}^4\mathrm{He} \rightarrow {}^7\mathrm{Be} + \gamma \end{cases}$$

$$IV\begin{cases} {}^7\mathrm{Be} + e^- \rightarrow {}^7\mathrm{Li} + \nu \\ {}^7\mathrm{Be} + p \rightarrow {}^8\mathrm{B} + \gamma, \end{cases}$$

the second reaction is weakened relative to the first, fewer ^{8}B neutrinos will result. Yet, there is reasonable agreement among laboratory measurements of these cross sections, and among theoretical prescriptions for extrapolating these measurements to the low energies characteristic of the solar interior. Likewise existing differences in opacity calculations by independent groups are too small to account for the ^{37}Cl discrepancy.

A more exciting possibility is that a fundamental physics flaw exists in the standard solar model. The ^{8}B neutrino flux (and, to a lesser extent, the ^{7}Be flux) depends sensitively on the central temperature of the sun: a 5% reduction of the core temperature brings theory into agreement with the ^{37}Cl results. Thus it is interesting to consider models that can achieve this reduction while producing the observed solar luminosity. A few of the more popular possibilities are:

(1) Models with low heavy element ("low Z") abundances in the solar core.[15] Such models abandon the assumption of the standard model that the initial heavy element abundances in the sun's interior can be equated to today's surface abundances.

An adjustment of the standard model fractional heavy element abundance from Z $\cong$ 0.02 to Z$\cong$ 0.002 reduces the core opacity, suppressing the ^{8}B and ^{7}Be neutrino fluxes and yielding a ^{37}Cl capture rate in agreement with Davis's measurements. The attractiveness of low-Z models is due in part to the existence of mechanisms for adding heavier elements to the sun's surface. These include the infall of comets and other debris, as well as the accumulation of dust as the sun passes through interstellar clouds. The increased radiative energy transport in low-Z models leads to thin convective zones, in contradiction to interpretations of the 5-minute solar surface oscillations.[16] A low He mass fraction also results. Furthermore Michaud, noting that diffusion of material from a thin convective envelope into the interior would deplete heavy elements at the surface, has questioned whether present abundances could accumulate in low-Z models.[17] Finally, the general consistency of solar heavy element abundances with those observed in other main sequence stars has discredited low-Z models.

(2) Models with hydrogen mixing into the core by turbulent diffusion.[18] The strength of this diffusion is proportional to a pseudo-Reynolds number Re* that, if assigned a strength on the order of 100, reduces the ^{37}Cl capture rate to the Davis value. However, the periods of certain solar oscillation eigenmodes (the low-frequency, low-degree gravity modes) may limit Re* to very moderate values ($\sim$ 25).[19]

(3) Models with convective mixing of the solar core.[20] If the mixing occurs sufficiently rapidly to maintain a homogeneous hydrogen abundance but sufficiently slowly to permit ^{3}H equilibration, the largest suppression in the ^{37}Cl capture rate is achieved. It is unclear whether such "slow mixing" models are compatible with the evolutionary sequences of old stars.

(4) Models where the innermost 20% of the solar mass periodically mixes.[21] For a period of several million years (approximately the Kelvin time of the solar core) following mixing the usual relationship between the observed surface luminosity and the rate of energy (and neutrino) production in the core will be altered: for this period there is no longer an equilibrium between the rates of solar energy production and energy emission from the surface. Calculations show that both the luminosity and high-energy ^{8}B neutrino flux are suppressed for a period after mixing. The spacing and duration of terrestrial ice ages have been linked to the time scales governing mixing and the subsequent return to equilibrium, and an instability in certain g-mode oscillations has been suggested as a possible trigger for mixing. Thus the Davis ^{37}Cl result is attributed to today being a "special time", near the close of the Pleistocene epoch.

Possible thermal or nuclear instabilities that might trigger sudden mixing have been investigated.[22] None of these studies has found unstable modes for standard solar models. Linear analyses have shown that the sun is stable against spherical thermal instabilities[23], non-spherical thermal instabilities[24], and nuclear reaction network instabilities at constant density and temperature.[25]

(5) Models in which the sun's central magnetic field is so strong that $|B|^2/8\pi$ is a

few percent of the gas pressure.[26] This contradicts the assumption in the standard model that hydrostatic equilibrium is achieved by balancing the gravitational force against the gas pressure gradient. It is believed that such intense fields could not persist over the lifetime of the sun. Another possibility is a rapidly rotating solar core, so that centripetal forces help support the sun.[27] However, the resulting solar oblateness would exceed the observed value.

(6) Perhaps some new particle physics is an essential ingredient of the solar model. One of the more interesting suggestions of this sort is the existence of wimps, weakly interacting massive particles.[28] A narrow window of masses and coupling strengths appears to exist which avoids laboratory constraints, yet allows a simultaneous solution of the solar neutrino and missing mass puzzles. In the sun wimps act as an additional mechanism for transporting energy out of the core and into the cooler solar mantle. A solar wimp "halo" is accumulated as cosmological wimps scatter as they pass through the sun, becoming trapped in the sun's gravitational field. If, as a wimp passes through the sun, the expected number of inelastic scatterings is ~1, then the wimp can be "heated" as passes through the core and later deposit that energy in the cooler outer regions of the sun through a second scattering.

Finally, there is the possibility that the standard solar model correctly describes solar neutrino production, but that some new particle physics phenomenon is altering the neutrinos before they reach earth. One possibility is the decay of the ν_e, though it has been appreciated for some time that the ν_e mass limit ($\lesssim 9$ eV) would then demand an unexpectedly large decay amplitude. Now that 150,000-year-old $\bar{\nu}_e$'s have been detected from SN1987A, it becomes exceedingly difficult to make this work.

A more intriguing possibility is neutrino oscillations.[29,30] The requirement for vacuum oscillations to occur is that at least one neutrino is massive and that the neutrino emitted in β decay, the current eigenstate, is not a state of definite mass (i.e., it is not an eigenstate of the free Hamiltonian). In gauge theories such a scenario is highly plausible: we know of no fundamental argument requiring the neutrinos to be massless, and the occurrence of flavor mixing in the quark section makes similar mixing among the leptons natural in unified theories. In the simple case of two mass eigenstates, the probability for observing a solar neutrino as an electron neutrino a distance L (in meters) from the sun is

$$P_{\nu_e} = 1 - \sin^2 2\theta_v \sin^2\left[\frac{1.27(m_2^2 - m_1^2)L}{E}\right] \underset{L\to\infty}{\longrightarrow} 1 - \frac{1}{2}\sin^2 2\theta_v$$

where E is the neutrino energy (in MeV), θ_v is the vacuum mixing angle, and m_1 and m_2 are the neutrino masses (in eV). The resulting extraordinary L/E ratio for solar neutrinos implies a sensitivity to extremely small masses, $m_2^2 - m_1^2 = \delta m^2 \gtrsim$

$10^{-12}\mathrm{eV}^2$, provided the mixing angle is reasonably large. In many grand unified theories a neutrino mass is generated of the form

$$m_\nu \sim M_D^2/M_R$$

where M_D is a quark or charged lepton mass (1MeV - 1 GeV) and M_R is some large mass of the theory. Thus experiments sensitive to $\delta m^2 \sim 10^{-12} eV^2$ could uncover new physics governed by mass scales $M_R \sim (10^9 - 10^{15})$GeV.

For many years it was believed that oscillations were an unlikely explanation of the solar neutrino puzzle. As the ^{37}Cl discrepancy is a factor of three, complete mixing of three neutrino species is required. This seems a priori quite improbable, and contrasts with the quark sector, where the mixing angles are small. [There is, however, the exception of "just so" oscillations[30], where the oscillation length ~ the earth-sun separation, so that two species with $\theta_v = \pi/4$ can completely interfere at earth for some typical solar neutrino energy.]

This situation changed in 1985 when Mikheyev and Smirnov showed that the density dependence of the neutrino effective mass, a phenomenon first discussed by Wolfenstein, could greatly enhance flavor oscillations of solar neutrinos: a ν_e is adiabatically converted to a ν_μ as it traverses a level crossing at some critical density.[1] The result is a range of neutrino mass differences δm^2 and vacuum mixing angles $\sin^2 2\theta_v$ for which this phenomenon could account for the ^{37}Cl results.

Consider the case of two flavor eigenstates related to the mass eigenstates through a vacuum mixing angle θ_v.

$$|\nu_e> = \cos\theta_v|\nu_1> + \sin\theta_v|\nu_2>$$
$$|\nu_\mu> = -\sin\theta_v|\nu_1> + \cos\theta_v|\nu_2>$$

If one writes the neutrino wave function in matter as

$$|\nu(x)> = a_e(x)|\nu_e> + a_\mu(x)|\nu_\mu>$$

where x is the radial coordinate in the sun, one obtains (after a suitable linearization of the Dirac equation)

$$i\frac{d}{dx}\begin{pmatrix} a_e \\ a_\mu \end{pmatrix} = \frac{1}{4E}\begin{pmatrix} 2\sqrt{2}G_F\rho(x) - \delta m^2\cos 2\theta_v & \delta m^2 \sin 2\theta_v \\ \delta m^2 \sin 2\theta_v & -2\sqrt{2}G_F\rho(x) + \delta m^2 \cos 2\theta_v \end{pmatrix}\begin{pmatrix} a_e \\ a_\mu \end{pmatrix} \quad (1)$$

where $\rho(x)$ is the solar density of electrons, the variable that determines the difference in the ν_e and ν_μ effective masses. It is convenient to rewrite Eq. (1) in a basis consisting of the local mass eigenstates (i.e., the states that diagonalized the right-hand side of Eq. (1))

$$|\nu_L(x)> = \cos\theta(x)|\nu_e> - \sin\theta(x)|\nu_\mu>$$

$$|\nu_H(x)> = \sin\theta(x)|\nu_e> + \cos\theta(x)|\nu_\mu>$$

when the local mixing angle is defined by

$$\sin 2\theta(x) = \frac{\sin 2\theta_v}{\sqrt{X^2(x) + \sin^2 2\theta_v}}$$

$$\cos 2\theta(x) = \frac{-X(x)}{\sqrt{X^2(x) + \sin^2 2\theta_v}} \tag{2}$$

where $X(x) = 2\sqrt{2}G_F\rho(x)E/\delta m^2 - \cos 2\theta_v$. Thus $\theta(x)$ ranges from θ_v to $\pi/2$ as the density $\rho(x)$ goes from 0 to ∞.

Defining

$$|\nu(x)\rangle = a_H(x)|\nu_H(x)> + a_L(x)|\nu_L(x)>$$

Eq. (1) becomes

$$i\frac{d}{dx}\begin{pmatrix} a_H \\ a_L \end{pmatrix} = \begin{pmatrix} \lambda(x) & i\alpha(x) \\ -i\alpha(x) & -\lambda(x) \end{pmatrix}\begin{pmatrix} a_H \\ a_L \end{pmatrix} \tag{3}$$

with the local mass eigenstate splitting determined by

$$\lambda(x) = \frac{\delta m^2}{4E}\sqrt{X^2(x) + \sin^2 2\theta_v}$$

while the mixing between the local mass eigenstates depends on the gradient of the density

$$\alpha(x) = \sqrt{2}\frac{E}{\delta m^2}\frac{\sin 2\theta_v}{(X^2(x) + \sin^2 2\theta_v)}G_F\frac{d}{dx}\rho(x).$$

The resulting physics is illustrated in Fig. 1. For a small mixing angle θ_v, one has $|\nu_e> \sim |\nu_L(x)>$ and $|\nu_\mu> \sim |\nu_H(x)>$ in vacuum, while at very high densities $|\nu_e> \sim |\nu_H(x)>$ and $|\nu_\mu> \sim |\nu_L(x)>$. Eq. (3) tells us that, if $|\alpha(x)| \ll 2\lambda(x)$ everywhere, an electron neutrino will remain on the heavy mass eigenstate trajectory if it is initially produced in a region of very high density. Thus the adiabatic conversion[2] $|\nu_e> \to |\nu_\mu>$ can be almost complete for a neutrino that travels from the center of the sun to the surface.

Of course, it may be that the adiabatic condition $|\alpha(x)| \ll \lambda(x)$ is not satisfied everywhere: this condition is clearly most stringent at the level crossing point, that value of x where the diagonal elements of Eq. (1) become degenerate and the splitting between the local mass eigenstates in Eq. (3) achieves its minimum value, $\delta m^2 \sin 2\theta_v/2E$. As $\alpha(x)$ depends on the gradient of $\rho(x)$, one must then extend the adiabatic approximation described above, which depends only on the initial and

final values of $\rho(x)$, to include the constraint that $\frac{d\rho(x)}{dx}$ not change too rapidly in the region of the crossing point.

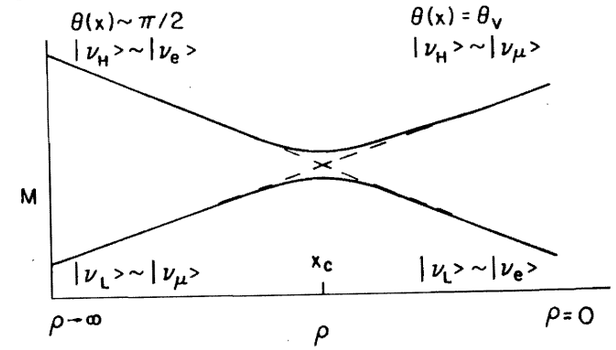

Figure 1. Schematic illustration of the MSW level crossing. The dashed lines correspond to the diagonal matrix elements H_{ee} and $H_{\mu\mu}$ on the right-hand side of Eq. (1). The solid lines are the corresponding heavy and light eigenvalues $\pm\lambda(x)$ of Eq. (3). If an electron neutrino is produced deep in the solar core and propagates adiabatically, it will follow the heavy-mass trajectory, emerging from the sun as a ν_μ.

Following Landau and Zener this can be done by solving Eq. (1) exactly for a linear density "wedge", as illustrated in Figure 2. The initial and final densities for the wedge are chosen to be the physical values (i.e., $\rho(x_i)$ is equated to the electron density in the solar core, and $\rho(x_f) = 0$). This builds in the adiabatic approximation result in that limit. The slope of the wedge is chosen to match the gradient of the solar density at the crossing point: this parameter should govern possible nonadiabatic behavior near the level crossing. The resulting solution of Eq. (1) can then be written in terms of parabolic cylinder functions, and is called the finite Landau-Zener approximation.[32]

However, because the nonadiabatic behavior is generally confined to the region around the crossing point, one can derive a simpler, but still very accurate result. The density wedge is extended, as illustrated by the dotted lines in Fig. 2, to $\pm\infty$. Under the assumption that the evolution in the regions of unphysical density is adiabatic, the exact solution in the physical region can be recovered by choosing the boundary conditions.

$$a_L(-\infty) = -a_\mu(-\infty) = \cos\theta(x_i)e^{-i\int_{-\infty}^{x_i}\lambda(x')dx'}$$

$$a_H(-\infty) = a_e(-\infty) = \sin\theta(x_i)e^{-i\int_{-\infty}^{x_i}\lambda(x')dx'}$$

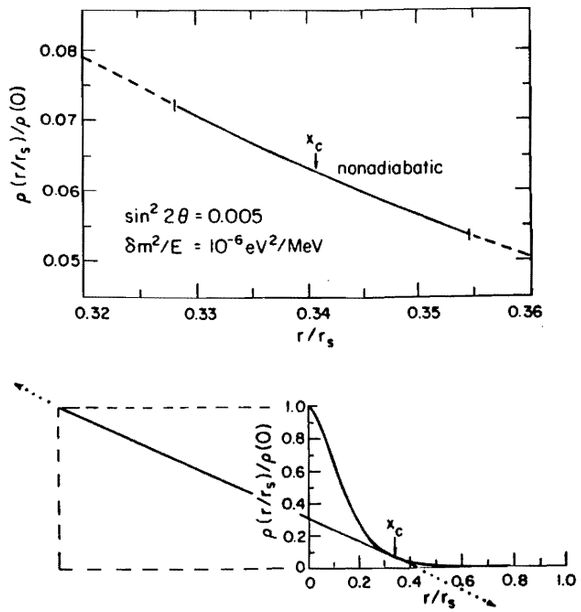

Figure 2. The top figure illustrates, for one choice of $\sin^2 2\theta$ and δm^2, that the region of nonadiabatic propagation (solid line) is usually confined to a narrow region about the crossing point x_c. In the lower figure, the solid lines represent the solar density $\rho(x)$ and a linear approximation to $\rho(x)$ that has the correct initial and final densities and the correct slope at x_c. The MSW equation can be solved analytically on this finite wedge (Ref. 32). By extending the wedge to $\pm\infty$ (dotted lines and arrows) and assuming adiabatic propagation in the regions of unphysical density, one obtains the simple Landau-Zener result of Eq. (4).

This allows one to evaluate the parabolic cylinder functions in their asymptotic limit. The result is the Landau-Zener formula for the electron survival probability a long distance from the sun,

$$P^{LZ}_{\nu_e} = \frac{1}{2} + \frac{1}{2}\cos 2\theta_v \cos 2\theta(x_i)\left(1 - 2e^{-\pi\gamma_c/2}\right) \tag{4}$$

where the adiabatic parameter γ_c is

$$\gamma_c = \frac{\lambda(x_c)}{|\alpha(x_c)|} = \left(\frac{\delta m^2}{2E}\right)^2 \frac{\sin^2 2\theta}{|\sqrt{2}G_F \frac{d}{dx}\rho(x_c)|} \tag{5}$$

where x_c is the radial coordinate at the crossing point. In the limit $\gamma_c \to \infty$, Eq. (4) reduces to the adiabatic result. The factor $2e^{-\pi\gamma_c/2}$ thus describes a hopping probability[3] from the heavy mass trajectory in Fig. 2 to the light mass trajectory.

Strong conversion $\nu_e \to \nu_\mu$ requires both that the neutrino passes through a "crossing point" at a critical density ρ_c

$$2\sqrt{2}G_F\rho_c E/\delta m^2 = \cos 2\theta$$

and that the crossing be at least somewhat adiabatic

$$\gamma_c \gtrsim 1.$$

The combination of these constraints, illustrated in Fig. 3, defines a triangle of interesting parameters in the $\frac{\delta m^2}{E} - \sin^2 2\theta_v$ plane, as Mikheyev and Smirnov first found numerically.

One can envision superimposing the spectrum of solar neutrinos, plotted as a function of 1/E and weighted by the response of the ^{37}Cl detector, on Fig. 3. Since Davis sees <u>some</u> solar neutrinos, the solutions must correspond to the boundaries of the triangle in Fig. 3. The horizontal boundary indicates the maximum $\frac{\delta m^2}{E}$ for which the sun's central density is sufficient to cause a level crossing. If a spectrum properly straddles this boundary, we obtain a result consistent with the Homestake experiment in which low energy neutrinos (large 1/E) lie above the level-crossing boundary (and thus remain ν_e's), but the high-energy neutrinos (small 1/E) fall within the unshaded region where strong conversion takes place. Thus such a solution would mimic nonstandard solar models in that only the ^{8}B neutrino flux would be strongly suppressed. The diagonal boundary separates the adiabatic and nonadiabatic regions. If the spectrum staddles this boundary, we obtain a second solution in which low energy neutrinos lie within the conversion region, but the high-energy neutrinos (small 1/E) lie below the conversion region and are characterized by $\gamma \ll 1$ at the crossing density. (Of course, the boundary is not a sharp one, but is characterized by the exponential of Eq. (4)). Such a nonadiabatic solution is quite distinctive since the flux of pp neutrinos, which is strongly constrained in the standard solar model and in any steady-state nonstandard model by the solar luminosity, would now be sharply reduced. An experimental confirmation of such a depletion would then demand new particle physics of the type under discussion here.

One can perform a more detailed calculation by including the finite extent of the neutrino-producing solar core (thereby permitting double level-crossings to

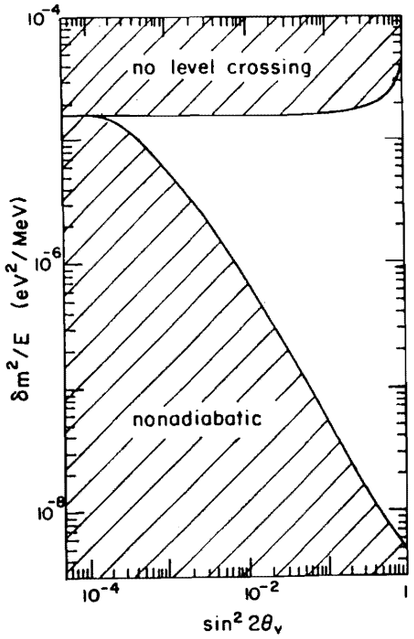

Figure 3. The shaded areas define those values of $\delta m^2/E$ and $\sin^2 2\theta_v$ that, for a neutrino produced at the sun's center, fail to satisfy the level-crossing condition (above the horizontal boundary) or the adiabatic condition ($\gamma_c \lesssim 1$, below the diagonal boundary). The conversion $\nu_e \to \nu_\mu$ if efficient in the unshaded region.

occur for some neutrinos produced on the far side of the sun); the details of response of the ^{37}Cl detector; and the uncertainties in the standard solar model predictions of the various neutrino fluxes. Those $\delta m^2 - \sin^2 2\theta$ consistent with the ^{37}Cl results, under the assumption of two-flavor MSW oscillations, are then given by the shaded region in Fig. 4. In addition to the cases discussed above, there is an allowed large-θ_v solution where matter effects and large vacuum oscillations combine to produce the necessary flux suppression.

The energy-dependent distortions of the solar-neutrino spectrum are a distinctive aspect of the MSW mechanism. We also see that this mechanism can generate, for the case of flavor oscillations, strong ν_μ/ν_τ fluxes. Thus the development of

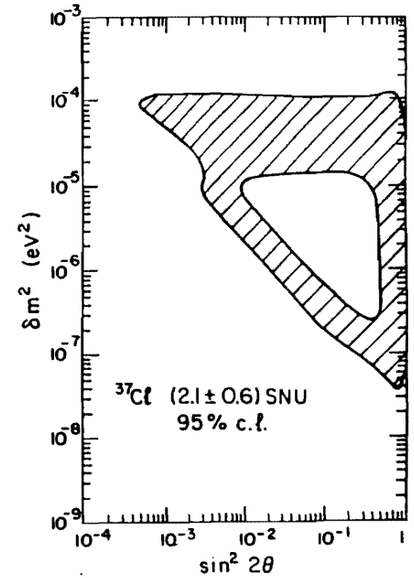

Figure 4. For the assumption of two-flavor neutrino oscillations, values of δm^2 and $\sin^2 2\theta_v$ outside the shaded region are excluded at 95% c.l. by the results of the ^{37}Cl experiment. The remaining allowed regions correspond to the level-crossing boundary (horizontal strip), adiabatic boundary (diagonal strip), and the large-vacuum-angle solution (vertical strip).

detectors with good spectral sensitivity and with strong neutral current signals has become an essential experimental issue.

Results from the Kamioka II water detector Cerenkov verify that the ^{8}B neutrino flux is less than the standard solar model prediction and, because the $\nu_e + e \to \nu_e + e$ scattering is forward-peaked, show the solar origin of the observed flux. This detector has operated with thresholds of 9.3 and 7.5 MeV, and thus is sensitive only to the high-energy tail of the ^{8}B flux. The result[14]

$$< \sigma\phi >= (0.46 \pm 0.05(\text{stat}) \pm 0.06(\text{sys})) < \sigma\phi >_{\text{SSM}}$$

is about a factor of two below the standard solar model prediction. This experiment

also has some spectral sensitivity since the recoil spectrum of the scattered electrons is recorded.

Analyses of the combined constraints from the ^{37}Cl and Kamioka II experiments have been performed by Bahcall and Haxton and, more recently (and using the most recent Kamioka II results) by Gates *et al.*[33] The allowed values of δm^2 and $\sin^2 2\theta_v$ determined in the latter calculation lie in the diagonal (for $\delta m^2 \lesssim 10^{-6}$ eV^2) and large-vacuum-angle ($\delta m^2 \lesssim 10^{-5}$ eV^2) parts of the MSW triangle.

Preliminary results are available from the SAGE (Soviet - American Gallium Experiment) detector. While the SSM prediction for the ^{71}Ga capture rate is approximately 130 SNU, the more significant aspect is the "minimum astronomical value" of 78 SNU.[34] That is, the large pp neutrino contribution guarantees a counting rate of at least this much, given standard weak interaction physics, provided only that the solar model burns in hydrostatic equilibrium. The SAGE result[35]

$$< \sigma\phi > \lesssim 79 \text{ SNU } 90\% \text{ c.l.}$$

is thus just marginally consistent with the minimum astronomical value, though the experimentalists stress that this limit depends on the assumption that the stable Ge tracer efficiency is giving the true efficiency for recovering ^{71}Ge atoms. Calibration of the SAGE detector by a neutrino source clearly will be an important direct test of ^{71}Ge extraction procedures. The preliminary best-value counting rate for the SAGE detector is about 20 SNU. If this result persists and is verified by the GALLEX[36] collaboration, it would seem to require new particle physics. This conclusion could be confirmed by new experiments, such as the heavy-water Cerenkov detector under construction at the Sudbury Neutrino Observatory, designed to detect heavy-flavor neutrinos and measure the characteristic MSW distortions of the ^{8}B neutrino spectrum.

It is possible that a low gallium counting rate, even in the simplest case of oscillations between two neutrino flavors, may not demand a unique MSW solution. Results[37] of combining the ^{37}Cl constraints with various hypothesized SAGE/GALLEX rates are shown in Fig. 5. For gallium counting rates above 20 SNU, two separate regions in the $\delta m^2 - \sin^2 2\theta$ plane would be consistent with both experiments. Provided the gallium rate is not too large each solution would also be compatible with present Kamioka II results. One of these solutions lies along the diagonal leg of the MSW triangle (the adiabatic boundary), the other in the large vacuum angle region. However for very low gallium counting rates ($\lesssim$ 20 SNU), these solutions coalesce into one region in the small-δm^2 portion of the diagonal solution.

Finally I would like to turn to a controversial aspect of the ^{37}Cl experiment that has stimulated much theoretical speculation: maximum likelihood analyses indicate $\sim$ 1% probability that ^{37}Cl results would result from a solar neutrino signal that is constant in time.[38] There have been further speculations that the ^{37}Cl signal varies with a period of $\sim$10 years and is approximately anticorrelated with the solar

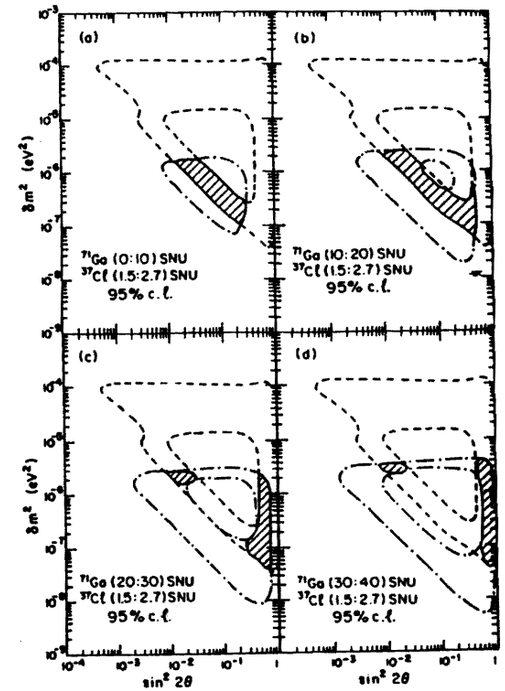

Figure 5. For the assumption of two-flavor neutrino oscillations, values of δm^2 and $\sin^2 2\theta$ outside the shaded regions are excluded at 95% c.l. when the ^{37}Cl results are combined with hypothetical ^{71}Ga counting rates.

cycle.[39] While there is no evidence for any time variations in the data from Kamioka II, these results are not sufficiently restrictive to contradict such a possibility.

There appear to be very few theoretical possibilities for generating such short-term solar neutrino flux variations. As Cisneros[4] originally suggested, a Dirac ν_{eL} with a nonzero magnetic moment could rotate, in the presence of the solar magnetic field, into a sterile ν_{eR}. Okun, Voloshin, and Vysotsky[5] revived and extended this

idea, pointing out that the effectiveness of the spin precession should track solar activity, so that an anticorrelation of the ν_e flux with the solar cycle could plausibly arise.

However, in the sun the degeneracy of the ν_{eL} and ν_{eR} is broken by their different matter interactions, suppressing the spin precession. Lim and Marciano[6] pointed out that this difficulty could be naturally circumvented for $\nu_{eL} \to \nu_{\mu R}$ transitions: the different matter interactions of the ν_e and ν_μ can compensate for the vacuum mass difference. The result, for a wide range of parameters, is a level crossing, analogous to the MSW effect, where the spin-flavor oscillation induced by an off-diagonal magnetic moment can occur at full strength between degenerate diagonal states.

This scenario has been studied[7] numerically by several authors, with the conclusion that interesting effects can arise if $B\mu_{\mu e} \gtrsim 10^{-6}\mu_B$ Gauss, where $\mu_B = e/2m_e$ and B is the solar magnetic field. This bound appears to push against limits in both particle and astrophysics. Stellar cooling rates for plasmon decay into $\nu\bar{\nu}$ place stringent limits[40] on magnetic moments μ_{ij} of light ($\lesssim 5$ keV) Dirac and Majorana (i $\neq$ j) neutrinos, $|\mu_{ij}| < 3 \cdot 10^{-12}\mu_B$. Even at this level it requires considerable theoretical artistry to generate a model μ_{ij} without introducing one-loop corrections to neutrino masses that are unacceptably large. In addition, one must postulate magnetic fields within the sun $\gtrsim 3 \cdot 10^5$ Gauss; these fields must be extensive, since the spin-flavor crossing point varies across the spectrum of solar neutrinos. Our direct knowledge of solar fields is derived from surface observations. While highly localized fields of $5 \cdot 10^3$ G have been seen within intense magnetic storms, the average surface field is on the order of a few G. Thus spin-flavor oscillations seem to require internal fields very much stronger and more extensive than any observed on the surface.

An alternative theoretical possibility that several authors have explored is the effect of solar density fluctuations: the adiabatic propagation of a neutrino mass eigenstate can be destroyed by a small perturbation if the frequency of that perturbation is close to the local oscillation frequency. The solar density fluctuations might change, in location, amplitude, or period, with the solar cycle, thereby producing a ν_e flux modulation consistent with Davis's data.

Schäfer and Koonin[41] numerically explored the effects of periodic density fluctuations on flavor oscillations. Changes linear in the fluctuation amplitude h were found for $h \sim .01$, a value they concluded was unrealistically large. Also, as the effect on $P_{\nu_e}(E_\nu)$ was primarily an oscillation about the unperturbed value, as E_ν was varied, little net change in the oscillation probability would remain for a spectrum of solar neutrinos. In contrast the large effects discussed later by Smirnov and Krastev[42] resulted in a general enhancement of P_{ν_e}, but arose for even more extreme amplitudes, $h \sim 0.1 - 0.2$.

Haxton and Zhang[43] recently offered a simple analytic description of the effects of density fluctuations, and also pointed out that solar currents could produce such effects in the absence of density fluctuations. The phenomenon, and its relationship

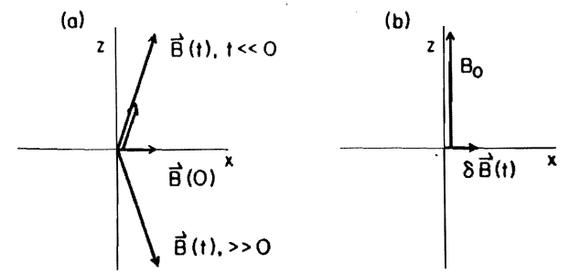

$\vec{B}(t) = B_x \hat{x} - B_z t \hat{z}$

$\vec{B}(t) = B_0 \hat{x} + \delta\vec{B}(t)$

$\delta\vec{B}(t) = \delta B(\hat{x}\cos\omega t + \hat{y}\sin\omega t)$

Figure 6. Atomic physics analogs of the MSW mechanism (a) and of periodic density perturbations or turbulence effects (b). The z-axis is the analog of flavor (up (down) corresponds to electron (muon) type), and similarly the two projections along the axis defined by the applied field $\vec{B}$ are the analog of the instantaneous mass eigenstates. In (a), reversal in $\vec{B}$ transforms a spin-up state into a spin-down state: the spin remains pointed along $\vec{B}$ if the change is made adiabatically. In (b), a rotating perturbation in the x-y plane of angular frequency ω will drive a spin reversal provided $\hbar\omega \sim 2\mu B_z$.

to the MSW effect, can be appreciated through the atomic physics analog illustrated in Fig. 6. The left-hand diagram illustrates an analog of the usual MSW effect. The two directions along the z-axis (up and down) correspond to the two neutrino flavors (electron and muon). Two directions along an applied magnetic field $\vec{B}(t)$ (parallel and antiparallel) correspond to the local or instantaneous mass eigenstates (heavy and light). $\vec{B}(t)$ evolves in time

$$\vec{B}(t) = B_x\hat{x} - B_z t\hat{z}$$

so that $\vec{B}$ is nearly parallel to $\hat{z}$ initially ($t \to -\infty$), but reverses itself as $t \to +\infty$. The magnitude of $\vec{B}(t)$ reaches a minimum at the "crossing point" $t = 0$.

The analogy with MSW neutrino oscillations is clear. A spin-up state will be converted into a spin-down state as t goes from $-\infty$ to $+\infty$ provided $\vec{B}(t)$ does not change too rapidly at the crossing point, where the splitting between the eigenstates $2\mu|\vec{B}|$ achieves its minimum value.

Now consider a different situation illustrated in the right-hand portion of Fig. 6. Again there is a strong magnetic field in the $\hat{z}$-direction, but in this case it is

static. To this is added a small, rotating perturbation in the x-y plane

$$\vec{B}_{\rm pert}(t) = \delta B(\hat{x}\cos\omega t + \hat{y}\sin\omega t)$$

where ω is a frequency that can be tuned to the difference between spin-up and -down unperturbed eigenstates. The resulting reversal of the spin direction is the phenomenon of adiabatic fast passage. It also illustrates the well-known exception to the adiabatic condition: if the perturbation is harmonic and in resonance, its effects grow linearly with time even though $\hbar\omega \gg \delta B$. The obvious neutrino oscillation analog suggests that a (nearly) harmonic density fluctuation (or turbulence pattern[43]) can have large effects provided it is resonant with the local oscillation frequency.

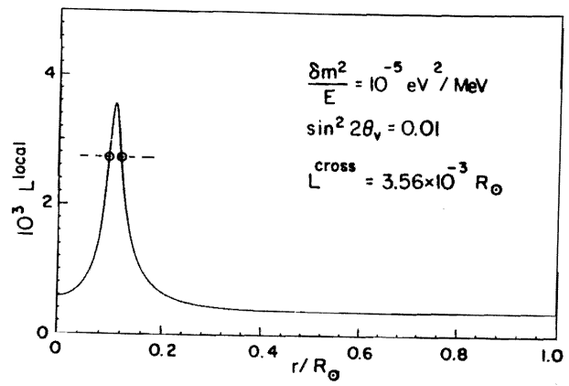

Figure 7. The local neutrino oscillation length in units of the solar radius $R_\odot$ as a function of the radial coordinate r, for $\delta m^2/E = 10^{-5}eV^2/MeV$ and $\sin^2 2\theta_v = 0.01$. The intersection with the dashed line illustrates two points where a perturbation of fixed oscillation length could lead to resonance.

The local oscillation length for one choice of δm^2 and $\sin^2 2\theta_v$ is shown in Fig. 7. The pattern is typical: the oscillation length varies greatly as the neutrino propagates, passing through a well-defined maximum at the crossing point. Therefore if there is a solar density/current perturbation of some characteristic frequency, the prospects for matching the local oscillation frequency at some density need not be small.

Furthermore the quantum mechanics in the case of solar neutrinos is quite rich. In general there will be two points of "stationary phase", which the neutrino

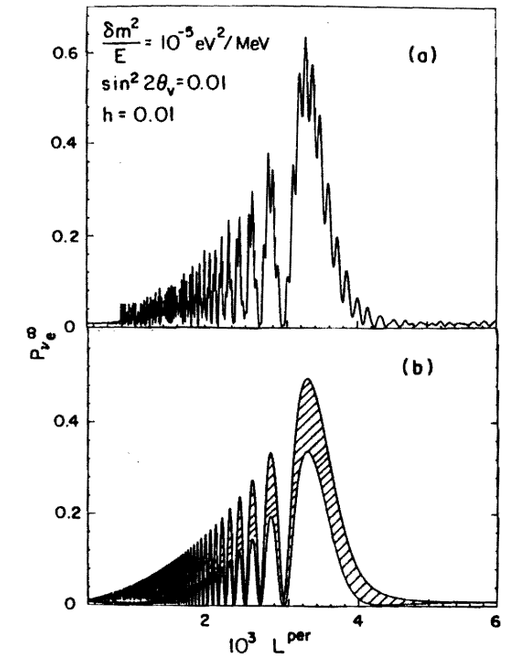

Figure 8. Neutrino survival probabilities for a highly adiabatic transition ($\gamma_c \sim 24$) with $\sin^2 2\theta = 0.01, \delta m^2/E = 10^{-5}eV^2/MeV$, and $h = 0.01$, with h the amplitude of an oscillatory perturbation (eddy currents or density fluctuations). Results are given as a function of the perturbation scale L^{per}, in units of $R_\odot$, for an exact integration (a) and for the approximate expression derived in Ref. 43. The band in the approximate calculation represents the region within which P_{ν_e} will oscillate, a feature apparent in (a). The oscillation length at crossing is $3.56 \cdot 10^{-3} R_\odot$.

encounters on entering and on leaving the resonance region. There will be phase interference between these separated regions of strong perturbation. If the stationary phase points are well separated, each region can be treated by a standard quadratic expansion. But if they approach one another, which occurs if the resonant frequency

is close to the frequency characterizing the crossing point, a more complicated expansion is required. Finally, the perturbation may be of some importance even if the length scale exceeds (somewhat) that characterizing the crossing point: that is, one must treat the "classically forbidden" region.

Haxton and Zhang showed that this problem could be attacked by using the uniform approximation, and that a very accurate solution exists which contains both the adiabatic and Landau-Zener results, in the appropriate limits, when the perturbation is turned off.[43]

Rather than present the detailed results, I show the numerical results in Figs. 8 and 9. The comparisons with exact calculations is impressive. Furthermore, dramatic effects clearly arise for small perturbations ($\delta\rho/\rho \sim 0.005 - 0.01$), and these effects persist over a range of perturbation frequencies and range of neutrino energies. Thus such density fluctuations, even if characterized by some band width rather than a fixed frequency, are capable of affecting a spectrum of neutrinos.

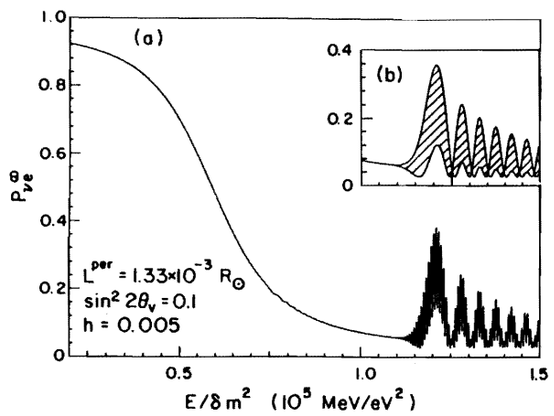

Figure 9. As in Fig. 8, only for $\delta m^2/E = 5 \cdot 10^{-5} eV^2/MeV, \sin^2 2\theta_v = 0.1$, and $h = 0.005$. The results are given as a function of neutrino energy.

Unlike other mechanisms for producing time variations in the solar neutrino flux, no new particle physics must be added to the MSW mechanism to generate such effects. This analog of adiabatic fast passage is simply another interesting manifestation of the effective neutrino mass in matter. Could the strength, frequency, or location of density perturbations or turbulence be tied to the solar cycle, thereby providing a plausible mechanism for periodic variations in the solar flux? At first

inspection this appears unlikely: the largest effects arise for highly adiabatic transitions, where crossings occur at high density. A simple connection with activity in the convective zone is not obvious in this case. However, it has been argued that turbulence at the base of the convective zone could generate g-mode excitation of large amplitude in the core, contradicting this naive conclusion.[44] In this case, such a mechanism for time variations might be more plausible than ones demanding both unusual particle physics (such as neutrino magnetic moments $\sim 10^{-12}\mu_B$) and unlikely solar physics (very large and extensive magnetic fields within the convective zone, $\sim 10^6 G$).

This work was supported in part by the U.S. Department of Energy, and by NASA under grant #NAGW-2523.

References

1. S.P. Mikheyev and A. Yu. Smirnov, *Yad. Fiz.* **42** (1985) 1441 [*Sov. J. Nucl. Phys.* **42** (1985) 913]; *Nuovo Cimento* **9C** (1986) 17. (More complete numerical results can be found in S.P. Rosen and J.M. Gelb, *Phys. Rev.* **D34** (1986) 969.) L. Wolfenstein, *Phys. Rev.* **D17** (1978) 2369 and **D20** (1979) 2634.
2. H. Bethe, *Phys. Rev. Lett.* **56** (1986) 1305; A. Messiah, in *Massive Neutrinos in Astrophysics and in Particle Physics*, Proceedings of the 21st Rencontre de Moriond, Tignes, France, 1986, ed. by O. Fackler and J. Tran Thanh Van (Edition Frontiéres, Gif-sur-Yvette, 1986).
3. W.C. Haxton, *Phys. Rev. Lett.* **57** (1986) 1271; S.J. Parke, *Phys. Rev. Lett.* **57** (1986) 1275.
4. A. Cisneros, *Astrophys. Space Sci.* **10** (1981) 87.
5. L.B. Okun, M.B. Voloshin, and M.I. Vysotsky, *Zh. Eksp. Teor. Fiz.* **91** (1986) 754 [*Sov. Phys. JETP* **64** (1986) 446]; *Yad. Fiz* **44** (1986) 677 [*Sov. J. Nucl. Phys.* **44** (1986) 440]; M.B. Voloshin and M.I. Vysotsky, *ibid* **44** (1986) 845 [**44** (1986) 544]; E. Kh. Akhmedov, *Phys. Lett.* **B213** (1988) 64; R. Barbieri and G. Fiorentini, *Nucl. Phys.* **B304** (1988) 909.
6. C.S. Lim and W.J. Marciano, *Phys. Rev.* **D37** (1988) 1368.
7. A.B. Balantekin, P.J. Hatchell, and F. Loreti, *Phys. Rev.* **D41** (1990) 3583; H. Minakata and H. Nunokawa, *Phys. Rev. Lett.* **63** (1989) 121.
8. J.N. Bahcall and R.K. Ulrich, *Rev. Mod. Phys.* **60** (1988) 297; J.N. Bahcall, W.F. Huebner, S.H. Lubow, P.D. Parker, and R.K. Ulrich, *Rev. Mod. Phys.* **54** (1982) 767.
9. See, for example, T.A. Tombrello and P.D. Parker, *Phys. Rev.* **131** (1963) 2582 and R.D. Williams and S.E. Koonin, *Phys. Rev.* **C23** (1981) 2773.
10. J.N. Bahcall, private communication.
11. S. Turck-Chiéze, S. Cohen, M. Cassé, and C. Doom, *Ap. J.* **335** (1988) 415; see S. Turck-Chiéze, in IAU Symposium 121. *Inside the Sun*, ed. G. Berthomieu and M. Cribier (Bordrecht, Kluwer), p. 125 for a discussion of a plasma opacity correction that increases the ^{37}Cl rate by 0.6 SNU over the 1988 value.

12. A. Garcia, E.G. Adelberger, P.V. Magnus, H.E. Swanson, O. Tengblad, and the ISOLDE collaboration.
13. C.W. Johnson, E. Kolbe, S.E. Koonin, and K. Langanke, W.K. Kellogg Radiation Laboratory, preprint MAP-140 (Fig. 1).
14. K.S. Hirata *et al.*, *Phys. Rev. Lett.* **63** (1989) 16 and **65** (1990) 1297.
15. J.N. Bahcall and R.K. Ulrich, *Ap. J* **170** (1971) 593; I. Iben, Jr., *Ann. Phys.* **54** (1969) 169.
16. E.L. Rhodes, Jr., R.K. Ulrich, and G.W. Simon, *Ap. J.* **28** (1977) 901; J. Christensen-Dalsgaard and D.O. Gough, *Nature* **288** (1980) 545.
17. G. Michaud, *Nature* **266** (1977) 433.
18. E. Schatzman and A. Maeder, *Nature* **290** (1981) 683; A. Maeder, in *Inside the Sun*, ed. G. Berthomieu and M. Cribier (Kluwer- Dordrecht, 1990), p. 133.
19. G. Berthomieu, J. Provost, and E. Schatzman, *Nature* **308** (1984) 254; various additional references are given in Maeder's article (Ref. 18).
20. D. Ezer and A.G.W. Cameron, *Astrophys. Lett.* **1** (1988) 1977; G. Shaviv and E.E. Salpeter, *Phys. Rev. Lett.* **21** (1968) 1602; J.N. Bahcall, N.A. Bahcall, and R.K. Ulrich, *Ap. J. Lett.* **2** (1968) 91.
21. F.W.W. Dilke and D.O. Gough, *Nature* **240** (1972) 262; W.A. Fowler, *Nature* **238** (1972) 24; E.J. Opik, *Contrib. Armagh. Obs.* No. 9 (1953).
22. R.L. Gilliland, *Ap. J.* **290** (1985) 344; I.W. Roxburgh, in *Solar Neutrinos and Neutrino Astronomy*, AIP Conf. Proc. No. 126, ed. M.L. Cherry, W.A. Fowler, and K. Lande (New York, 1985).
23. M. Schwarzschild and R. Harm, *Ap. J.* **184** (1973) 5.
24. M.N. Rosenbluth and J.N. Bahcall, *Ap. J.* **184** (1973) 9.
25. D.O. Gough, in *The Solar Output and its Variations*, ed. O.R. White (Boulder, Westview Press, 1985).
26. Z. Abraham and I. Iben, Jr., *Ap. J.* **170** (1971) 157; D. Bartenwerfer, *Astron. Astrophys.* **25** (1973) 455; E.N. Parker, *Astrophys. Space Sci.* **31** (1974) 261; R.K. Ulrich, *Ap. J.* **188** (1974) 369.
27. P. Demarque, J. Mengel, and A. Sweigart, *Ap. J.* **183** (1973) 997 and *Nature Phys. Sci.* **246** (1973) 33.
28. J. Faulkner and R.L. Gilliland, *Ap. J.* **299** (1985) 994; D.N. Spergel and W.H. Press, *Ap. J.* **294** (1985) 679.
29. B. Pontecorvo, Sov. Phys. JETP **53** (1967) 1717.
30. Z. Maki, N. Nakagawa, and S. Sakata, *Prog. Theor. Phys.* **28** (1962) 675.
31. S.L. Glashow and L.M. Krauss, *Phys. Lett.* **B190** (1987) 199; V. Barger, K. Whisnant, and R.J.N. Phillips, *Phys. Rev.* **D24** (1981) 538.
32. W.C. Haxton, *Phys. Rev.* **D35** (1987) 2352.
33. E. Gates, L.M. Krauss, and M. White, Yale Univ. preprint YCTP-P26-91.
34. J.N. Bahcall, B.T. Cleveland, R. Davis, Jr., and J.K. Rowley, *Ap. J. Lett.* **292** (1985) L79.
35. A.I. Abazov *et al.*, Phys. Rev. Lett. 67 (1991) 3332.

36. T. Kirsten, in *'86 Massive Neutrinos in Astrophysics and Particle Physics*, Proc. of the Sixth Moriond Workshop, ed. O. Fackler and J. Tran Thanh Van (Gif-sur-Yvette, Editions Frontiéres, 1986), p. 119.
37. J.N. Bahcall and W.C. Haxton, *Phys. Rev.* **D40** (1989) 931.
38. B.W. Filippone and P. Vogel, *Phys. Lett.* **B246** (1990) 546; J.N. Bahcall and W.H. Press, *Ap. J.* **370** (1991) 730; J.W. Bieber *et al.*, *Nature* (London) **348** (1990) 407; L.M. Krauss, *ibid.* **348** (1990) 403.
39. K. Lande and R. Davis, in Proc. of the 21st Int. Cosmic Ray Conference (Adelaide), ed. R.J. Protheroe (Graphic Services, Northfield, South Australia, 1990); G.A. Bazilevskaya *et al.*, *Yad. Fiz.* **39** (1984) 856 [*Sov. J. Nucl. Phys.* **39** (1984) 543].
40. G.G. Raffelt, *Phys. Rev. Lett.* **64** (1990) 2856.
41. A. Schäfer and S.E. Koonin, *Phys. Lett.* **B185** (1987) 417.
42. P.I. Krastev and A.Yu. Smirnov, *Phys. Lett.* **B226** (1989) 341.
43. W.C. Haxton and W.-M. Zhang, *Phys. Rev.* **D43** (1991) 2484.
44. See, for example, the paper by E. Schatzman in these proceedings.